Platelet-rich plasma was obtained by centrifugation, and diluted to $5 \times 10^5$ platelets per μl with plasma. Platelet aggregation was assayed as described[7]. An aortic ring 4 mm long was prepared from thoracic aorta and mounted on a pair of wires in an organ bath filled with Krebs–Henseleit buffer gassed with 95% $O_2$–5% $CO_2$ at 37 °C. Preload was 0.5 g. The ring was contracted with 0.1 μM noradrenaline and its relaxation response to various concentrations of cicaprost tested.

**Blood pressure, heart rate and bleeding time.** Basal blood pressure and heart rate were measured in conscious animals by using the tail-cuff method. In the analysis of cicaprost- or $PGE_2$-induced hypotension, animals were anaesthetized with pentobarbital sodium (60 mg $kg^{-1}$; i.p.), and arterial blood pressure was monitored through a cannula into the carotid artery. Bleeding time was measured as described[24].

**Prostanoid production.** Isolated aorta was preincubated in oxygenated Krebs–Henseleit buffer at 37 °C for 1 h and then incubated in fresh buffer for 20 min; the supernatant was assayed. Prostanoids in peritoneal lavage were extracted with Sep-Pak C18 columns and then assayed for 6-keto-$PGF_{1\alpha}$ and $PGE_2$ (ref. 25).

**Analysis of thrombus formation.** Mice (24–30 g) were anaesthetized with halothane and the carotid arteries exposed by a cervical incision. A piece of Parafilm 1 mm wide was inserted under the artery and 5 μl of a 7.5% $FeCl_3$ solution was dropped on the artery[10]. After 1 min the solution was wiped off, and the mice were allowed to recover from the anaesthetic. After 4 h, the arteries and blood flow were examined microscopically by cutting the distal end of the artery. A 5-mm long segment containing the affected region was excised and fixed with 10% formaldehyde. Thrombosis-induced death of animals treated with 5% $FeCl_3$ solution was recorded after 24 h.

**Inflammation.** Vascular permeability was tested using Pontamine skyblue as described[26]. PGs alone, bradykinin alone, or both were intradermally injected. After 40 min, mice were killed. The exuded dye in the skin was extracted and the amounts determined. Permeability was expressed as a percentage of that induced by 10 nmol bradykinin alone in the same animals. Carrageenin-induced pleurisy was evoked by injecting 40 μl of 2% carrageenin into the right pleural cavity of mice[14]. After 3 h, they were killed and the exudate volume measured.

**Nociceptive tests.** The tail-flick response was evoked either by heat[18] or by applying pressure[19]. Latencies were determined by using a tail-flick apparatus (Ugo Basile) and with an analgesy meter (Ugo Basile), respectively. In the hot-plate test, mice were placed on a plate (55 ± 0.1 °C) and the latency for jumping determined as described[18]. In the writhing test[20], mice were intraperitoneally injected with either 0.9% acetic acid (5 ml $kg^{-1}$) or PGs (2 μg). The frequency of stretch responses was counted for 30 min for acetic acid or for 15 min for PGs. Indomethacin (10 mg $kg^{-1}$) was administered intraperitoneally 30 min before acetic acid injection.

**Data analysis.** Data are expressed as means ± s.e.m.. The significance of difference between groups was evaluated using ANOVA with a subsequent Dunnett's test, except for thrombus formation (Fig. 2 legend).

Received 28 February; accepted 4 June 1997.


1. Campbell, W. B. & Halushka, P. V. in *The Pharmacological Basis of Therapeutics* (9th edn) (eds Hardman, J. G. *et al.*) 601–616 (McGraw-Hill, New York, 1996).
2. Bunting, S., Moncada, S. & Vane, J. R. The prostacyclin-thromboxane $A_2$ balance: pathophysiological and therapeutic implications. *Br. Med. Bull.* **39,** 271–276 (1983).
3. Davies, P., Bailey, P. J., Goldenberg, M. M. & Ford-Hutchinson, A. W. The role of arachidonic acid oxygenation products in pain and inflammation. *Annu. Rev. Immunol.* **2,** 335–357 (1984).
4. Ushikubi, F., Hirata, M. & Narumiya, S. Molecular biology of prostanoid receptors: an overview. *J. Lip. Mediat.* **12,** 343–359 (1995).
5. Namba, T. *et al.* cDNA cloning of a mouse prostacyclin receptor. *J. Biol. Chem.* **269,** 9986–9992 (1994).
6. Morham, S. G. *et al.* Prostaglandin synthase 2 gene disruption causes severe renal pathology in the mouse. *Cell* **83,** 473–482 (1995).
7. Armstrong, R. A. *et al.* Fucntional and ligand binding studies suggest heterogeneity of platelet prostacyclin receptor. *Br. J. Pharmacol.* **97,** 657–668 (1989).
8. Murata, T. *et al.* General pharmacology of beraprost sodium: Effect on the autonomic, cardiovascular and gastrointestinal systems, and other effects. *Arzneim. Forsch.* **39,** 867–876 (1989).
9. Huang, P. L. *et al.* Hypertension in mice lacking the gene for endothelial nitric oxide synthase. *Nature* **377,** 239–242 (1995).
10. Kurz, K. D., Main, B. W. & Sandusky, G. E. Rat model of arterial thrombosis induced by ferric chloride. *Thromb. Res.* **60,** 269–280 (1990).
11. Vadas, P., Wasi, S., Movat, H. Z. & Hay, J. B. Extracellular phospholipase $A_2$ mediates inflammatory hyperaemia. *Nature* **293,** 583–585 (1981).
12. Ferreira, S. H. Inflammatory pain, prostaglandin hyperalgesia and the development of peripheral analgesics. *Trends Pharmacol. Sci.* **2,** 183–186 (1981).
13. Winter, C. A. & Flataker, L. Reaction thresholds to pressure in edematous hindpaws of rats and responses to analgesic drugs. *J. Pharmacol. Exp. Ther.* **150,** 165–171 (1965).
14. Utsunomiya, I., Nagai, S. & Oh-ishi, S. Differential effects of indomethacin and dexamethasone on cytokine produciton in carrageenin-induced rat pleurisy. *Eur. J. Pharmacol.* **252,** 213–218 (1994).
15. Oida, H. *et al. In situ* hybridization studies of prostacyclin receptor mRNA expression in various mouse organs. *Br. J. Pharmacol.* **116,** 2828–2837 (1995).
16. Malmberg, A. B. & Yaksh, T. L. Hyperalgesia mediated by spinal glutamate or substance P receptor blocked by spinal cyclooxygenase inhibition. *Science* **257,** 1276–1279 (1992).
17. Oka, T., Aou, S. & Hori, T. Intracerebroventricular injection of interleukin-1β induces hyperalgesia in rats. *Brain Res.* **624,** 61–68 (1993).
18. Piercey, M. F. & Schroeder, L. A. Spinal and supraspinal sites for morphine and nefopam analgesia in the mouse. *Eur. J. Pharmacol.* **74,** 135–140 (1981).
19. Millan, M. J. & Colpaert, F. C. 5-Hydroxytryptamine (5-HT)$_{1A}$ receptors and the tail-flick response. II. High efficacy 5-$HT_{1A}$ agonists attenuate morphine-induced antinociception in mice in a competitive-like manner. *J. Pharmacol. Exp. Ther.* **256,** 983–992 (1991).
20. Koster, R., Anderson, M. & deBeer, E. J. Acetic acid for analgesic screening. *Fed. Proc.* **18,** 412 (1959). **FINAL PAGE?**
21. Doherty, N. S. *et al.* The role of prostaglandins in the nociceptive response induced by intraperitoneal injection of zymosan in mice. *Br. J. Pharmacol.* **91,** 39–47 (1987).
22. Vane, J. R., Anggard, E. E. & Botting, R. M. Regulatory functions of the vascular endothelium. *New Eng. J. Med.* **323,** 27–36 (1990).
23. Kawabe, T. *et al.* The immune responses in CD40-deficient mice: impaired immunoglobulin class switching and germinal center formation. *Immunity* **1,** 167–178 (1994).
24. Dejana, E., Callioni, A., Quintana, A. & Gaetano, G. Bleeding time in laboratory animals. II—A comparison of different assay conditions in rats. *Thromb. Res.* **15,** 191–197 (1979).
25. Ritter, J. M., Aksoy, A., Cragoe, E. J. & Taylor, G. W. Actions of amiloride analogues on prostacyclin synthesis by rat aortic rings. *Br. J. Pharmacol.* **92,** 857–862 (1987).
26. Ueno, A., Tokumasu, T., Naraba, H. & Oh-ishi, S. Involvement of bradykinin in endotoxin-induced vascular permeabiity increase in the skin of rats. *Eur. J. Pharmacol.* **284,** 211–214 (1995).


**Acknowledgements.** We thank K. Ishikawa and Y. Kataoka for ES cell injeciton and K. Okuyama for secretarial assistance. This work was supported by grants from the Ministry of Education, Science and Culture of Japan, the Japanese Society for Promotion of Sciences, the Uehara Memorial Foundation, the Smoking Research Foundation and the Japanese Foundation on Metabolism and Diseases.

Correspondence and requests for materials should be addressed to S.N. (e-mail: snaru@mfour.med.kyoto-u.ac.jp).

# Crustacean appendage evolution associated with changes in Hox gene expression

**Michalis Averof* & Nipam H. Patel†**

*Wellcome/CRC Institute, Tennis Court Road, Cambridge CB2 1QR, UK*
*† HHMI, University of Chicago, MC1028, N-101, 5841 South Maryland Avenue, Chicago, Illinois 60637, USA*
** Present address: EMBL, Meyerhofstrasse 1, 69117 Heidelberg, Germany*

**Homeotic (Hox) genes specify the differential identity of segments along the body axis of insects. Changes in the segmental organization of arthropod bodies may therefore be driven by changes in the function of Hox genes[1–3], but so far this has been difficult to demonstrate. We show here that changes in the expression pattern of the Hox genes *Ubx* and *AbdA* in different crustaceans correlate well with the modification of their anterior thoracic limbs into feeding appendages (maxillipeds). Our observations provide direct evidence that major morphological changes in arthropod body plans are associated with changes in Hox gene regulation. They suggest that homeotic changes[1,4] may play a role in the normal process of adaptive evolutionary change.**

Genetic manipulation of model organisms like *Drosophila* can reveal the potential of developmental systems to undergo particular types of morphological change: for example, patterns of segmental specialization may be altered by changing the function of Hox genes. This approach alone, however, cannot identify the actual genetic changes that take place over macro-evolutionary timescales. Comparative studies are required but these so far indicate that crustaceans and insects share almost identical complements of Hox genes[5] and that the domains of Hox gene expression have been broadly conserved during insect evolution (reviewed in ref. 6). Initial comparisons of Hox gene expression between crustaceans and insects documented changes associated with the independent specialization of trunk regions (thorax and abdomen) in these

animals[7,8]. Studies on such divergent animals are constrained by the lack of a common framework for morphological comparison. We focus here on comparisons between different subgroups of crustaceans, where we can identify changes in Hox gene expression that relate to well characterized variations in patterns of segmental specialization.

In most arthropods, thoracic appendages are specialized primarily for locomotor functions. But in some crustaceans, limbs from the anterior thorax have been recruited and specialized for the manipulation of food. These modified thoracic appendages, termed maxillipeds, are morphologically and functionally more similar to the feeding appendages (maxillae) of the more anterior gnathal segments than to the remaining thoracic limbs. Maxillipeds are generally reduced in size, show modification, fusion, or loss of particular limb elements, and are primarily associated with feeding, not locomotion[9–12]. These morphological specializations are reminiscent of partial homeotic transformations[4] (thoracic to gnathal) and represent the evolution of new and distinct segmental identities in the anterior region of the trunk. We investigated whether any of these changes could be associated with differences in Hox gene regulation by studying the combined expression of the Hox genes *Ubx* and *abdA* in diverse crustacean species. In crustaceans, these genes are thought to be involved in specifying the post-gnathal region of the trunk[7]. Using the monoclonal antibody FP6.87 (ref. 13), which recognizes a conserved epitope specific to the Ubx and AbdA proteins[7,13], we examined Ubx–AbdA expression in thirteen crustacean species from nine different orders. In all cases, we observed expression in the limb-bearing region of the trunk posterior to gnathal segments, or posterior to thoracic segments bearing maxillipeds when these were present.

In branchiopod crustaceans, which do not have maxillipeds, *Ubx* and *abdA* are expressed throughout the thoracic region. In *Artemia franciscana* (Anostraca), there is FP6.87 staining in a domain that starts from the first thoracic segment (T1) and extends posteriorly throughout the thorax[7] (Fig. 1a, b). This corresponds to a region of the body where all segments and the associated limbs develop similar morphological characteristics[7]. Expression patterns are similar in a related anostracan species (fairy shrimp; data not shown). In *Triops longicaudatus* (Notostraca), the same anterior boundary of Ubx–AbdA distribution is seen in the early larval stages, at a time when all thoracic limbs are morphologically identical and clearly distinct from the gnathal appendages (Fig. 1c–e).

A similar pattern of expression is also observed in leptostracans, a group of malacostracan crustaceans that bear no maxillipeds in anterior trunk segments. The thorax of all malacostracans consists characteristically of eight segments; leptostracans are thought to have retained a number of primitive malacostracan features, including uniform morphology of all eight thoracic segments and limbs[9] (Fig. 1f). In early embryos of *Paranebalia belizensis* (Leptostraca), we observed FP6.87 staining in the entire post-gnathal region of the trunk, starting from T1 (Fig. 1g). We consider this anterior boundary of *Ubx–abdA* expression to be primitive within malacostracans and shared by all crustaceans with primitively uniform thoracic segments (as also seen in branchiopods). Below we describe changes in *Ubx–abdA* expression in two groups of malacostracan crustaceans which carry different numbers of maxillipeds, peracarids and decapods.

In peracarids, the first, and sometimes second, of the eight thoracic segments bear limbs that have acquired several characteristics of feeding appendages. We find that the modification of these segments correlates with the repression of *Ubx–abdA* expression in those segments. In the mysid *Mysidium colombiae* (Mysida), the T1 limb has acquired the characteristic gnathal-like morphology of maxillipeds (Fig. 2a); a similar modification is seen in the most distal part of the T2 limb (Fig. 2a), although this limb still retains most morphological and functional characteristics of a swimming appendage. In comparison to leptostracans, the initial anterior

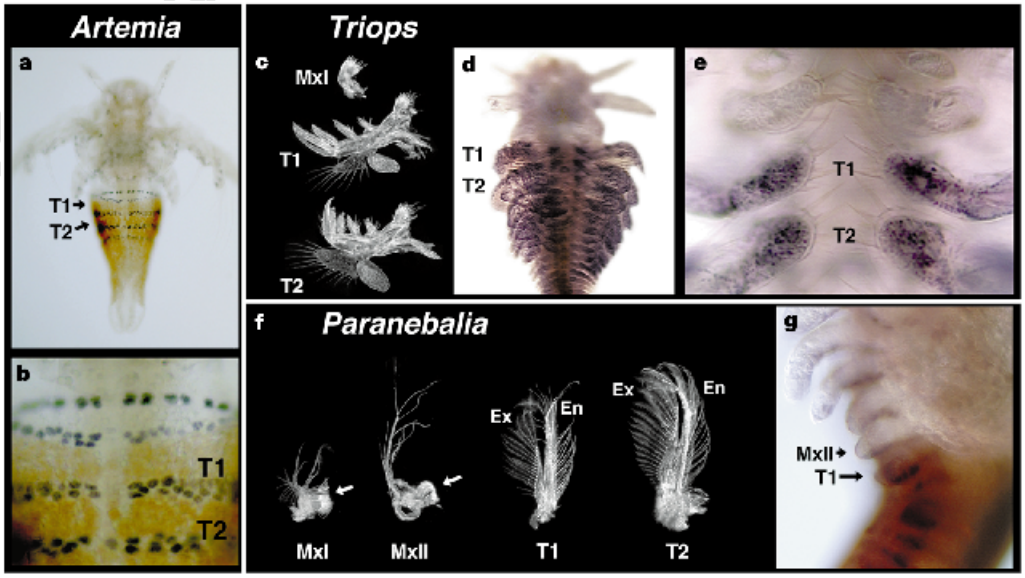


**Figure 1** Crustaceans with no maxillipeds. **a**, FP6.87 (brown) and engrailed (black) staining of *Artemia* before the morphological appearance of thoracic appendages. **b**, Higher-magnification view. *Ubx–abdA* expression begins in the first thoracic segment (T1) and extends into the more posterior regions. The anterior expression border is segmental, but will eventually extend to a slightly more anterior parasegmental border in the ventral neurogenic region[7]. **c**, Morphology of limbs in *Triops* larvae (3 days after hatching). Thoracic appendages (T1, T2) have similar morphology and are distinct from the appendages of gnathal segments (MxI is shown, MxII is reduced in size even further). **d**, FP6.87 staining of *Triops* (2.5 days after hatching). **e**, Higher-magnification view, focused on cells at the limb bases. As in *Artemia*, *Ubx–abdA* expression begins at the T1 segment and extends posteriorly. **f**, Morphology of adult limbs in *Paranebalia*. All eight thoracic appendages have similar morphology; T1 is somewhat smaller, particularly its exopod (Ex). Gnathal appendages have very reduced endopods and exopods, but prominent endites (arrows). **g**, FP6.87 (brown) and engrailed (black) staining of *Paranebalia* as limbs are becoming visible. *Ubx–abdA* expression begins in T1 and extends posteriorly.

boundary of *Ubx–abdA* expression in mysids appears to be shifted backwards by an entire metameric unit. There is no FP6.87 staining in the T1 limb, weak staining in T2, and stronger staining in the more posterior regions of the trunk (Fig. 2b, c). We investigated this expression in more detail at different developmental stages. At all stages, we observed the same anterior borders of expression. At very early stages, when parasegments are only two cells wide, *Ubx–abdA* appear to be expressed or repressed uniformly within any given metameric unit, in both ectoderm and mesoderm (see posterior segments in Fig. 2b). Uniform early expression, however, becomes modulated within individual metameres during later development (differences in the level of expression, mosaic patterns; Fig. 2c, d). It is interesting to note that *Ubx-abdA* are expressed in the proximal portion of the T2 endopod, but excluded from its more distal part (Fig. 2d); it is this distal part of the T2 endopod that acquires gnathal-like characteristics (Fig. 2a). We have observed similar domains of *Ubx-abdA* expression in two other peracarids, a gammarid amphipod and an asellote isopod; in both cases the appearance of maxillipeds on T1 correlates with the repression of *Ubx–abdA* expression in that segment (data not shown).

Decapods are generally described as having three pairs of maxillipeds and five pairs of walking limbs in their thorax (hence the name Decapoda)[9,12]. Many of those limbs, however, show extensive structural variation, both between species and within the same species at different developmental stages. We examined two decapod genera showing different patterns of segmental specialization in the anterior thorax. The cleaner shrimps *Periclimenes yucatanicus* and *Periclimenes pedersoni* (Decapoda) show the typical decapod reduction and modification of the three most anterior pairs of thoracic limbs during embryonic development (Fig. 3a) and into adulthood (Fig. 3b). FP6.87 staining indicates that *Ubx–abdA* expression is excluded from the first three thoracic parasegments and limbs, is weak in T4, and stronger in more posterior segments (Fig. 3c, d). Thus, with respect to leptostracans, the anterior boundary of Ubx–AbdA distribution appears to have shifted backwards by three metameric units. In the lobster *Homarus americanus* (Decapoda), the specialization of anterior thoracopods differs at embryonic and postembryonic stages. Adult lobsters have five pairs of large thoracic limbs (T4–T8) plus three pairs of reduced limbs (T1–T3; these are readily identifiable as maxillipeds). At hatching, however, only the T1 and T2 limbs appear to be distinctly reduced and similar to gnathal appendages. The T3 limb is morphologically similar to the more posterior walking legs and does not have the properties of a maxilliped (Fig. 3e). In *Homarus* embryos, FP6.87 staining is absent from the first two thoracic parasegments (including the T1 and T2 limbs), and strong in T3 and more posterior segments (Fig. 3f). Thus, the anterior boundary of embryonic expression of *Ubx-abdA* in *Homarus* appears to have shifted backwards by two metameric units relative to leptostracans, and corresponds to the morphological transition in thoracic limbs seen at hatching.

Maxillipeds are widely distributed among crustaceans and can also be found in non-malacostracan groups like copepods. We examined *Ubx–abdA* expression in two cyclopoid copepods, *Mesocyclops edax and Dioithona oculata* (Cyclopoida), both of which have a single pair of maxillipeds on T1 (Fig. 2e). Once again, this morphological arrangement appears to be associated with a posterior shift in Ubx–AbdA distribution: FP6.87 staining extends from T2 backwards, with no expression in the T1 limb, moderate expression in the T2 limb, and stronger expression further posterior (Fig. 2f). We observed a similar expression pattern in a diaptomid calanoid copepod (data not shown).

Collectively, our observations reveal a striking correlation between the expression of *Ubx–abdA* and the morphological specialization of corresponding segments. In particular, the repression of *Ubx* and *abdA* expression in anterior trunk segments is associated with the development of a gnathal-like identity in those segments. Bearing in mind the widely documented role of Hox genes in specifying segmental identity[1,14,15], we suggest that this association may be direct and causal. A similar correlation between regional vertebral morphology and Hox expression has been reported among different species of vertebrates[16,17]; in that case,

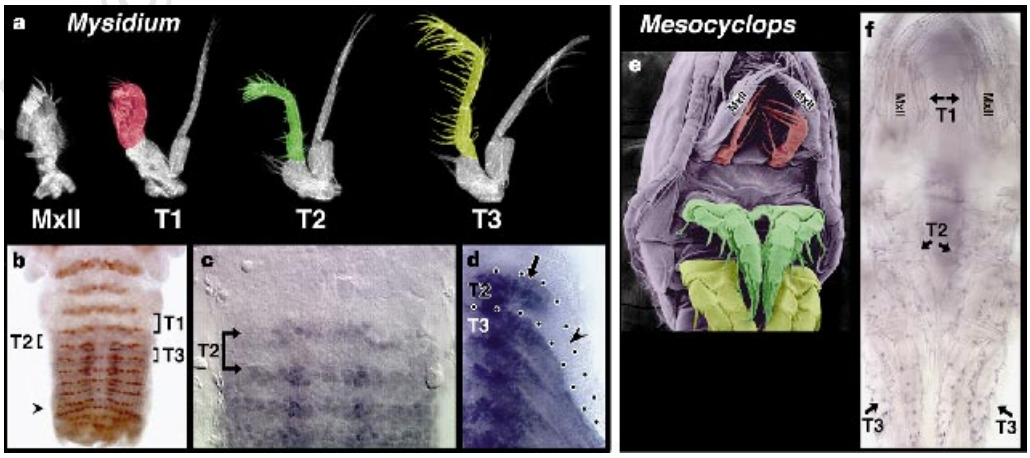


**Figure 2** Crustaceans with one pair of maxillipeds. **a**, Morphology of adult limbs in *Mysidium*. MxII is second maxillary appendage; portions of the endopods of the first, second and third thoracic appendages (T1, T2 and T3) are shown in red, green and yellow respectively; thoracic exopods are the long right-most branches. The T1 limb is similar to that of gnathal appendages (as shown in MxII), with prominent endites and a reduction in particular elements of the endopod. The T2 limb has a 'mosaic' endopod, with a distal portion that resembles gnathal limbs and a proximal portion that resembles more posterior thoracic limbs. T3 to T8 limbs have similar morphology. **b**, FP6.87 (black) and engrailed (brown) staining during early *Mysidium* development. Staining is absent from T1, weak in T2, and strong in T3 and more posteriorly. Arrowhead marks T8, which at this stage is only 2 cells wide and shows uniform FP6.87 staining. **c**, FP6.87 staining in *Mysidium* at a slightly later time. Expression can be seen extending to the parasegment boundary in the more medial (neurogenic) region of posterior T1. At this stage FP6.87 staining shows modulated levels of expression within segments. **d**, FP6.87 staining in developing *Mysidium* limbs. In the T2 limb (outlined with dots), staining is seen in the proximal (black arrow) but not the distal (black arrowhead) portion of this limb; contrast this to the same portions of the T3 limb. **e**, Scanning electron micrograph of adult *Mesocyclops*. Limbs are colour-coded as in **a**. Maxillipeds on T1 are morphologically similar to gnathal appendages (MxII) and quite distinct from the remaining thoracic limbs (T2 shown). **f**, FP6.87 staining of larval stage of *Mesocyclops*. Nuclear staining appears punctate owing to the distant spacing of ectodermal cells in these mature copepod limbs.

however, the observed changes appear to be associated primarily with regional changes in vertebral numbers, not with the evolution of new vertebral identities.

Maxilliped-bearing segments presumably acquire their distinct identity by expressing different combinations, patterns, or amounts of homeoproteins than do the other thoracic or gnathal segments. Studies in *Drosophila* have highlighted the importance of fine intrasegmental (mosaic) modulation in the expression patterns of Hox genes—it appears that different decisions on regional identity can be taken independently by different groups of cells within a segment[15,18,19]. The identity of a maxilliped-bearing segment could therefore be determined as a mosaic, with some parts of the segment retaining a thoracic identity and others becoming homeotically transformed to a gnathal fate. The spatially modulated distribution of Ubx–AbdA within the mysid T2 limb (Fig. 2d) and the resulting mosaic morphology of this appendage (Fig. 2a) are consistent with this hypothesis. In addition to spatial modulation, temporal changes in the expression of Hox genes are important because different decisions on regional identity can be taken at different developmental times[18–20]. Our results indicate that it is the early patterns of *Ubx–abdA* expression (before and during the initial phases of limb growth) that correlate with the modification of anterior thoracic limbs into feeding appendages. Later changes in expression patterns are observed in *Artemia*[7] and *Paranebalia* (data not shown), where *Ubx–abdA* expression appears to retract from anterior thoracic segments as these segments mature. In both species this correlates with a reduction in the relative size of the corresponding thoracic limbs (Fig. 1f). Perhaps more interesting are cases like *Triops* and *Homarus*, where qualitative changes in the structure of anterior limbs can be seen during larval life. The late expression patterns of Hox genes in those species are not yet known.

The fossil record suggests that primitive crustaceans had a rather uniform series of thoracic segments, with no apparent specialization of anterior thoracic limbs[21–23]. Specialization of anterior thoracic appendages, however, is widespread among crustaceans today, and the phylogenetic distribution of these specializations suggests that similar morphological transformations have occurred independently several times during crustacean evolution (Fig. 4). Maxillipeds, for example, appear to have arisen independently in crustacean groups as diverse as malacostracans, copepods and

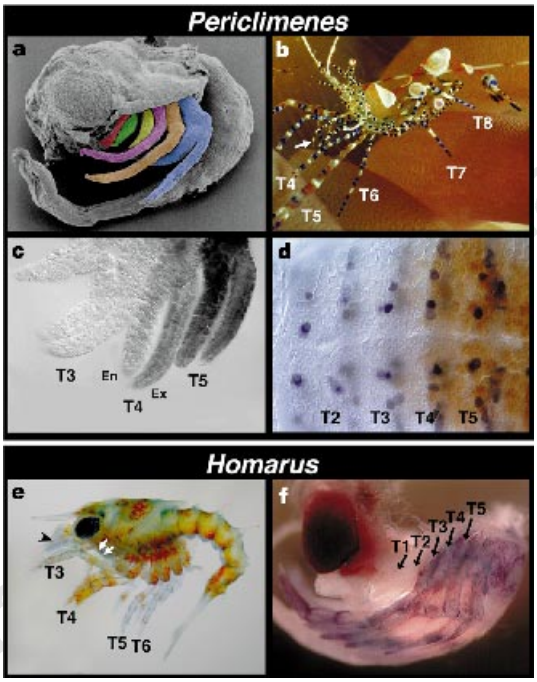


**Figure 3** Crustaceans with several pairs of maxillipeds. **a**, Scanning electron micrograph of late *Periclimenes yucatanicus* embryo showing the reduced size of the T1, T2 and T3 appendages (red, green and yellow respectively; T4 is pink, T5 is orange, T6 is blue, T7 and T8 are hidden more medially). **b**, Adult *P. yucatanicus* showing typical decapod morphology, with five pairs of walking legs (T4–T8) and three pairs of maxillipeds (T1–T3); arrow indicates the position of maxillipeds–only the T3 pair is clearly visible here. **c**, FP6.87 staining of developing *P. yucatanicus* limbs shows that staining is absent from T3 and more anterior limbs, weak in the T4 limb (En is endopod, Ex is exopod), and stronger in T5 and more posterior limbs. **d**, FP6.87 (brown) and engrailed (black) staining in developing neuromeres of *P. yucatanicus*; staining is weak in posterior T3 and anterior T4, and stronger more posteriorly. **e**, *Homarus* larvae 24 h after hatching. T3 is a well developed limb and is morphologically similar to more posterior walking legs. The maxillipeds of T1 and T2 are too small to be visible but their position is indicated by white arrowheads; grey arrowhead marks the antennal appendages. **f**, FP6.87 staining of *Homarus*; staining begins in T3 and extends posteriorly.

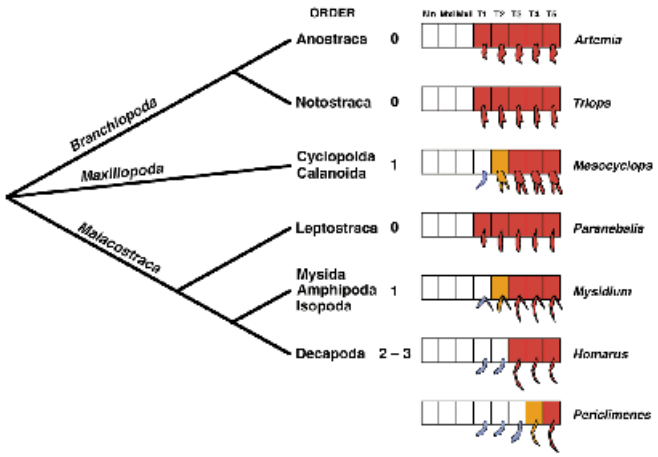


**Figure 4** Phylogenetic distribution of different patterns of segmental specialization and Ubx–AbdA expression among crustaceans. For each of the nine orders examined, we indicate the number of maxillipeds (0, 1, 2 or 3), and illustrate the different thoracic morphologies and segmental domains of Ubx–AbdA expression (dark orange for strong staining, light orange for weaker staining, and white for no staining) seen during early embryonic development. In each drawing three gnathal segments are depicted, followed by the first five thoracic segments. Maxillipeds are shown in blue, gnathal appendages are not shown. In each case, the early embryonic pattern of *Ubx–abdA* expression correlates with the eventual morphology of the thoracic segments; maxillipeds appear on those thoracic segments that do not express *Ubx–abdA*. The phylogenetic relationship of the three classes described here (Branchiopoda, Maxillopoda and Malacostraca) remains unresolved[11,12]. The ancestral crustacean body plan probably lacked maxillipeds, as did the ancestral malacostracan body plan[9,11,21–23].

remipedes[9,11]. Our findings indicate that such convergent changes may have been achieved by similar developmental changes (involving similar posterior shifts in the expression boundary of *Ubx–abdA*) on several independent occasions. This suggests that, given a particular developmental system, there may be limited ways for achieving a particular morphological result.

It is often thought that the study of development mechanisms can provide a rigorous way to assess the homologous or convergent origin of morphological characteristics (see refs 7, 16, 24 for example). Our observations introduce one complication: this expectation will be true only in the extent to which convergent events are driven by distinguishable genetic changes. In this respect, it will be interesting to establish whether the observed convergent shifts in Hox expression can be attributed to distinguishable changes at a fine molecular-genetic level. □

### Methods

The monoclonal antibody against Ubx and AbdA (FP6.87) is described in ref. 13; the monoclonal antibodies against Engrailed (4D9 and 4F11) are described in ref. 25. Immunochemical staining is described in refs 25, 26. Cuticularized embryos and larvae were sonicated briefly to allow efficient penetration of reagents[26]. Further details on collection, rearing, fixation, sonication and staining are available upon request.

Received 25 March; accepted 10 June 1997.


1. Lewis, E. B. A gene complex controlling segmentation in *Drosophila*. *Nature* **276,** 567–570 (1978).
2. Raff, R. A. & Kaufman, T. C. *Embryos, Genes, and Evolution* (Indiana University Press, Bloomington, 1991).
3. Akam, M., Dawson, I. & Tear, G. Homeotic genes and the control of segment diversity. *Development* **104** (suppl.), 123–133 (1988).
4. Bateson, W. *Materials for the Study of Variation, Treated with Especial Regard to Discontinuity in the Origin of Species* (Macmillan, London, 1894).
5. Averof, M. & Akam, M. *HOM/Hox* genes of *Artemia*: implications for the origin of insect and crustacean body plans. *Curr. Biol.* **3,** 73–78 (1993).
6. Averof, M., Dawes, R. & Ferrier, D. Diversification of arthropod *Hox* genes as a paradigm for the evolution of gene functions. *Sem. Dev. Cell. Biol.* **7,** 539–551 (1996).
7. Averof, M. & Akam, M. *Hox* genes and the diversification of insect and crustacean body plans. *Nature* **376,** 420–423 (1995).
8. Panganiban, G., Sebring, A., Nagy, L. & Carroll, S. The development of crustacean limbs and the evolution of arthropods. *Science* **270,** 1363–1366 (1995).
9. Calman, W. T. *Crustacea* (Black, London, 1909).
10. Giesbrecht, W. in *Handwörterbuch der Naturwissecschaften* (ed. Dittler, R.) 800–840 (Fischer, Jena, 1931).
11. Schram, F. R. *Crustacea* (Oxford University Press, Oxford, 1986).
12. Brusca, R. C. & Brusca, G. J. *Invertebrates* 1–922 (Sinauer, Sunderland Massachusetts, 1990).
13. Kelsh, R., Weinzierl, R. O. J., White, R. A. H. & Akam, M. Homeotic gene expression in the locust *Schistocerca*: an antibody that detects conserved epitopes in *Ultrabithorax* and *Abdominal-A* proteins. *Dev. Genet.* **15,** 19–31 (1994).
14. McGinnis, W. & Krumlauf, R. Homeobox genes and axial patterning. *Cell* **68,** 283–302 (1992).
15. Akam, M. *Hox* genes and the evolution of diverse body plans. *Phil. Trans. R. Soc. Lond. B* **349,** 313–319 (1995).
16. Burke, A. C., Nelson, C. E., Morgan, B. A. & Tabin, C. Hox genes and the evolution of vertebral axial morphology. *Development* **121,** 333–346 (1995).
17. Gaunt, S. J. Conservation in the Hox code during morphological evolution. *Int. J. Dev. Biol.* **38,** 549–552 (1994).
18. Castelli-Gair, J., Greig, S., Micklem, G. & Akam, M. Dissecting the temporal requirements for homeotic gene function. *Development* **120,** 1983–1995 (1994).
19. Castelli-Gair, J. & Akam, M. How the Hox gene *Ultrabithorax* specifies two different segments: the significance of spatial and temporal regulation within metemeres. *Development* **121,** 2973–2982 (1995).
20. Salser, S. J. & Kenyon, C. A. *C. elegans* Hox gene switches on, off, on, and off again to regulate proliferation, differentiation, and morphogenesis. *Development* **122,** 1651–1661 (1996).
21. Briggs, D. E. G. The morphology, mode of life, and affinities of *Canadaspis perfecta* (Crustacea, Phyllocarida), Middle Cambrian, Burgess Shale, British Columbia. *Phil. Trans. R. Soc. Lond. B* **281,** 439–487 (1978).
22. Muller, K. J. & Walossek, D. External morphology and larval development of the Upper Cambrian maxillopod *Bredocaris admirabilis*. *Foss. Strat.* **23,** 1–70 (1988).
23. Walossek, D. The Upper Cambrian *Rehbachiella* and the phylogeny of Branchiopoda and Crustacea. *Foss. Strat.* **32,** 1–202 (1993).
24. Wagner, G. P. The biological homology concept. *Annu. Rev. Ecol. Syst.* **20,** 51–69 (1989).
25. Patel, N. H., Kornberg, T. B. & Goodman, C. S. Expression of *engrailed* during segmentation in grasshopper and crayfish. *Development* **107,** 201–212 (1989).
26. Patel, N. H. in *Methods in Cell Biology, 44.* Drosophila Melanogaster: *Practical Uses in Cell Biology* (eds Goldstein, L. S. B. & Fyrberg, E.) 445–487 (Academic, New York, 1994).


**Acknowledgements.** We thank M. Akam and F. Ferrari for discussion; K. Rützler and the Smithsonian Institution for hosting our collecting expeditions at Carrie Bow Caye in Belize; R. White for the FP6.87 antibody; G. Wyngaard for *Mesocyclops*; E. Chang for *Homarus* embryos; M. Sepanski for help with electron microscopy; A. Crittenden and L. Brown for technical assistance; and M. Palopoli, R. Chasan and S. Cohen for comments on the manuscript. This work was supported by the Wellcome Trust (M.A.), the Carnegie Institution of Washington, and the Howard Hughes Medical Institute (N.H.P.).

Correspondence and requests for materials should be addressed to N.H.P. (e-mail: npatel@midway.uchicago.edu).

# Recruitment of functional $GABA_A$ receptors to postsynaptic domains by insulin

**Q. Wan*, Z. G. Xiong†, H. Y. Man*, C. A. Ackerley*, J. Braunton*, W. Y. Lu†, L. E. Becker*, J. F. MacDonald† & Y. T. Wang***

** Divisions of Pathology and Neuroscience, Hospital for Sick Children, and Departments of Pathology and † Physiology, University of Toronto, Toronto, Ontario M5G 1X8, Canada*

**Modification of synaptic strength in the mammalian central nervous system (CNS) occurs at both pre- and postsynaptic sites[1,2]. However, because postsynaptic receptors are likely to be saturated by released transmitter, an increase in the number of active postsynaptic receptors may be a more efficient way of strengthening synaptic efficacy[3–7]. But there has been no evidence for a rapid recruitment of neurotransmitter receptors to the postsynaptic membrane in the CNS. Here we report that insulin causes the type A γ-aminobutyric acid ($GABA_A$) receptor, the principal receptor that mediates synaptic inhibition in the CNS[8], to translocate rapidly from the intracellular compartment to the plasma membrane in transfected HEK 293 cells, and that this relocation requires the β2 subunit of the $GABA_A$ receptor. In CNS neurons, insulin increases the expression of $GABA_A$ receptors on the postsynaptic and dendritic membranes. We found that insulin increases the number of functional postsynaptic $GABA_A$ receptors, thereby increasing the amplitude of the $GABA_A$-receptor-mediated miniature inhibitory postsynaptic currents (mIPSCs) without altering their time course. These results provide evidence for a rapid recruitment of functional receptors to the postsynaptic plasma membrane, suggesting a fundamental mechanism for the generation of synaptic plasticity.**

We used quantitative electron-microscopic analysis of immunogold labelling to investigate translocation of $GABA_A$ receptors in HEK 293 cells stably expressing the α1, β2 and γ2 subunits of rat $GABA_A$ receptors[9], the most common subunit combination of native $GABA_A$ receptors in the mammalian CNS[10]. We found that, under control conditions, only a small number of immunogold-labelled β2 subunits could be observed at the membrane surface, and that most labelling was localized intracellularly (Fig. 1a,c). Treatment with insulin dramatically increased the number of gold-labelled $GABA_A$ receptor subunits in the plasma membrane (Fig. 1b,c); the change could be detected as early as 10 min after insulin treatment (data not shown). An increase in receptor synthesis was not involved, as even 60 min of insulin treatment did not affect the total cellular expression of β2 subunits (Fig. 1c). Pretreatment of cells with genistein, a membrane-permeable inhibitor of protein-tyrosine kinases[11,12], prevented the insulin-induced translocation without altering basal $GABA_A$ receptor distribution (Fig. 1c), suggesting a requirement for activation of the insulin receptor tyrosine kinase[13]. To determine whether the insulin-induced receptor translocation leads to an increase in the number of functional $GABA_A$ receptors on the plasma-membrane surface, we recorded $GABA_A$ receptor-mediated whole-cell currents in these cells. Bath application of insulin (0.5 μM) produced a significant increase in the amplitude of the currents, an effect not observed in cells pretreated with genistein (Fig. 1d). These results demonstrate a rapid increase in the number of functional $GABA_A$ receptors on the plasma-membrane surface as a result of receptor translocation by activation of insulin-receptor tyrosine kinase.

To determine which subunit(s) is required for insulin-induced